Journal of Chromatography A, 1523 (2017) 127–139

Contents lists available at ScienceDirect

Journal of Chromatography A

journal homepage: www.elsevier.com/locate/chroma

Capillary electrophoresis–mass spectrometry for direct structural identification of serum N-glycans

Christa M. Snyder[a,1], Xiaomei Zhou[a,1], Jonathan A. Karty[a], Bryan R. Fonslow[b], Milos V. Novotny[a], Stephen C. Jacobson[a,*]

[a] Department of Chemistry, Indiana University, Bloomington, IN 47405-7102, United States
[b] SCIEX Separations, Brea, CA 92821, United States

ARTICLE INFO

Article history:
Received 1 May 2017
Received in revised form 1 September 2017
Accepted 3 September 2017
Available online 9 September 2017

Keywords:
Microchip electrophoresis
Capillary electrophoresis
Mass spectrometry
N-glycan
Glycomics
Sialic acid

ABSTRACT

Through direct coupling of capillary electrophoresis (CE) to mass spectrometry (MS) with a sheathless interface, we have identified 77 potential N-glycan structures derived from human serum. We confirmed the presence of N-glycans previously identified by indirect methods, e.g., electrophoretic mobility standards, obtained 31 new N-glycan structures not identified in our prior work, differentiated co-migrating structures, and determined specific linkages on isomers featuring sialic acids. Serum N-glycans were cleaved from proteins, neutralized via methylamidation, and labeled with the fluorescent tag 8-aminopyrene-1,3,6-trisulfonic acid, which renders the glycan fluorescent and provides a −3 charge for electrophoresis and negative-mode MS detection. The neutralization reaction also stabilizes the labile sialic acids. In addition to methylamidation, native charges from sialic acids were neutralized through reaction with 4-(4,6-dimethoxy-1,3,5-triazin-2-yl)-4-methylmorpholinium to amidate α2,6-linked sialic acids in the presence of ammonium chloride and form lactones with α2,3-linked sialic acids. This neutralization effectively labels each type of sialic acid with a unique mass to determine specific linkages on sialylated N-glycans. For both neutralization schemes, we compared the results from microchip electrophoresis and CE.

1. Introduction

Protein glycosylation patterns are sensitive to changes in physiology as a result of various types of cancer [1–4]. Additionally, glycomic profiling has proved to be a powerful tool for differentiating among healthy individuals and patients with different types of cancer by multiple methods (e.g., mass spectrometry [5–18], microchip electrophoresis [19–23] and capillary [24–31] electrophoresis). Determination of specific N-glycan structures contributing to disease state differentiation is essential to understanding biological pathways of both cancer and glycosylation. Identification of disease-relevant N-glycan structures allows these structures and their abundances to be monitored on a variety of different platforms.

Capillary and microchip electrophoresis generates high resolution separations which can resolve both linkage and positional isomers [19,21,22,29–31]; however, the separation method alone lacks structural information. Several techniques, such as electrophoretic mobility standards or glucose unit analysis [32,33], have been previously employed in an attempt to correlate information across data sets from different devices and samples, but these techniques are limited by the resolution of the separations and standards available. Mass-spectrometric detection gives direct mass and structural information, but often struggles to resolve isomers without extensive fragmentation [34–37], which requires analytes to be in high abundance [38]. Our previous work used a combination of microchip electrophoresis and matrix-assisted laser desorption/ionization-mass spectrometry (MALDI-MS) of well-characterized glycoproteins to identify N-glycan structures present in serum. We assigned electrophoretic mobilities to these structures and possible isomers in electropherograms by matching the electrophoretic mobilities of known N-glycans (referred to as electrophoretic mobility standards) to the electrophoretic mobilities of unknown structures [39,40].

Although this combination of techniques resulted in the assignment of N-glycan structures to 52 peaks, several N-glycans exhibited nearly identical electrophoretic mobilities, seen as a single peak [39]. Additionally, limited isomer information can be obtained from the correlation of electrophoretic mobility to molecular weight because structural and linkage isomers will have the same mass. The identification of isomers is, therefore, limited

* Corresponding author.
E-mail address: jacobson@indiana.edu (S.C. Jacobson).
[1] These authors contributed equally to this work.

http://dx.doi.org/10.1016/j.chroma.2017.09.009
0021-9673/

to enzymatic or MS^n studies. Enzymatic studies [37] are sometimes inconclusive because the enzymes lack sufficient specificity and reactions do not always go to completion, which results in incomplete characterization of a set of structures. The direct interfacing of capillary electrophoresis with mass spectrometry (CE-MS) [41–45] brings together high resolution separations and unambiguous structural identification. Several commercial options now exist to couple CE instrumentation to mass spectrometers in a facile and reproducible manner.

In an effort to obtain direct structural information about N-glycans present in serum, we used CE-MS to identify 77 potential N-glycan structures present in serum and to differentiate several co-migrating species. This study also led to identification of an additional 31 N-glycan structures, not observed in our prior work with microchip electrophoresis or MALDI-MS. Moreover, the importance of sialic acid isomers [46] led us to incorporate a selective charge neutralization strategy to separate α2,3 and α2,6 linkage isomers on both the microchip and capillary electrophoresis platforms. We previously neutralized native charges on N-glycans due to sialic acids through methylamidation [47], but 4-(4,6-dimethoxy-1,3,5-triazin-2-yl)-4-methyl-morpholinium chloride (DMT-MM) [48–50] selectively amidates α2,6 linkages in the presence of ammonium chloride and forms lactones with α2,3 linkages without any further treatment. This differentiation further aids in resolving structures in electrophoretic separations and also allows different linkage isomers to be identified by mass spectrometry [51].

2. Materials and methods

2.1. Materials

The following materials were used: ammonium chloride from Amresco; acrylamide and sodium dodecyl sulfate (SDS) from Bio-Rad Laboratories, Inc.; ammonium hydroxide from J.T. Baker; high-purity 8-aminopyrene-1,3,6-trisulfonic acid (APTS) from Beckman Coulter, Inc.; HPLC grade water and trifluoroacetic acid (TFA) from EMD Chemicals, Inc.; sodium hydroxide from Fisher Scientific; peptide-N-glycosidase F (PNGase F) of *Chryseobacterium menigosepticum* (EC 3.2.2.18) from ProZyme (GKE-5006A); Nonidet P-40 from Roche Diagnostics; activated carbon and amino (NH_2) micro-spin columns and 1000 Da cutoff cellulose dialysis tubes from Harvard Apparatus; ammonium acetate, hydrogen peroxide, hydrochloric acid, and isopropyl alcohol (IPA) from Macron Fine Chemicals; HPLC grade acetonitrile from Mallinckrodt Baker; tetrahydrofuran (THF) from VWR; Microposit MF-319 developer from MicroChem Corp.; chromium etchants 8002-A and 1020 and buffered oxide etchant from Transene Co., Inc.; 353NDT epoxy from Epoxy Technology; and B270 mask blanks and cover plates from Telic Co. All other chemicals were purchased from Sigma-Aldrich Co. Human serum samples were purchased from BioreclamationIVT.

2.2. Preparation of N-glycan samples

N-Glycans were enzymatically cleaved from standard glycoproteins (200 μg) and human serum (5 μL) with PNGase F and purified [52]. For enzymatic cleavage, samples were suspended in 10 μL phosphate buffer (pH 7.5) with 0.2% β-mercaptoethanol and 0.1% SDS and thermally denatured at 60 °C for 60 min. The solution was cooled to room temperature prior to the addition of a 1-μL aliquot of 10% Nonidet P-40 and was allowed to equilibrate for 5–10 min at room temperature. A 0.5-μL aliquot of PNGase in phosphate buffer was subsequently added to the solution, and the reaction mixture was then incubated overnight at 37 °C. For methylamidation of sialic acids on N-glycans [47], we modified the protocol to minimize sample loss and maximize purity [39].

Samples requiring no further treatment or derivatization were labeled with APTS [53] by established procedures [21] to impart a negative charge for electrophoresis and negative mode MS analysis and a fluorescent tag for detection. N-glycans were labeled with APTS by adding a 2-μL aliquot of 100 μM APTS solution prepared in 0.9 M citric acid and a 1-μL aliquot of 1 M sodium cyanoborohydride prepared in DMSO. The reaction was allowed to proceed for 4 h at 55 °C. The derivatization mixture was dialyzed overnight at room temperature with a 1000-Da cut-off cellulose membrane to reduce the amount of unreacted APTS in the sample.

2.3. Lactonization and amidation reaction and purification

Samples not neutralized by methylamidation were neutralized by amidation and spontaneous lactone formation with a slight modification of previously reported methods [51]. Briefly, 4-(4,6-dimethosy-1,3,5-triazin-2yl)-4-methylmorpholinium chloride (DMT-MM) was synthesized [54] by reacting 2 mL of N-methylmorpholine with 2.9 g of 2-chloro-4,6-dimethoxy-1,3,5-triazine in 60 mL THF and stirring at room temperature for 45 min. The precipitate was filtered, thoroughly washed with additional THF, and dried overnight in a vacuum desiccator. Cleaved, purified, and dried N-glycans were dissolved in 10-μL aliquots of 0.5 M DMT-MM in 0.5 M ammonium chloride solution at pH 6.5 and incubated at 60 °C for a minimum of 17 h. The neutralized N-glycans were recovered with graphite micro-spin columns [51]. After sample loading, columns were washed twice with 200 μL of 97:3 water/acetonitrile solution. Neutral glycans were then eluted by the addition of two 200-μL aliquots of 75:25 water/acetonitrile solution, and acidic glycans were subsequently eluted with two 200 μL aliquots of 75:25:0.1 water/acetonitrile/TFA. The samples were dried before labeling with APTS [21,53].

2.4. CE-ESI–MS

A bare-fused silica capillary cartridge (30 μm i.d. × 90 cm length; Opti-MS, SCIEX Separations) was conditioned according to manufacturer protocols before use in the CESI 8000 instrument (SCIEX Separations). In brief, the capillary was sequentially flushed for 10 min at 100 psi with methanol, 0.1 M NaOH, 0.1 M HCl, water, and 7.5 mM ammonium acetate with 10% IPA at pH 4.5 or 0.1% formic acid with 10% IPA at pH 2.8 (background electrolyte, BGE). The conductive side capillary was rinsed for a total of 9 min at 100 psi with methanol, water, and BGE before use. Dried samples were reconstituted in 20–50 μL 1:10 BGE:water prior to analysis, depending on initial sample amount. Hydrostatic injections at 1–5 psi for 5–30 s were used to introduce analytes to the capillary before a separation voltage of 24 or 30 kV was applied. Typically, a constant 2 or 3 psi was applied to the separation capillary to provide stable fluid flow for the electrospray. The capillary was interfaced with the nanospray source of an LTQ Orbitrap mass spectrometer (Thermo Fisher) through the provided adapter kit, and data acquisition was started through a contact closure relay. Electrospray was initiated by applying 1.2–1.6 kV for 5–30 s, then stepping the potential down to 1.0–1.45 kV (i.e., 100–150 V lower for stable electrospray) for the remainder of the separation through the Xcalibur software (Version 2.2, Thermo Fisher). Data were collected in negative ion mode over a range of 150–2000 m/z at the normal scan speed with 15 K resolution and the FTMS analyzer. Collision-induced dissociation (CID) MS/MS scans were obtained with the FTMS analyzer for more abundant species and ITMS for lower intensity analytes at a normalized collision energy of 35 (q = 0.25).

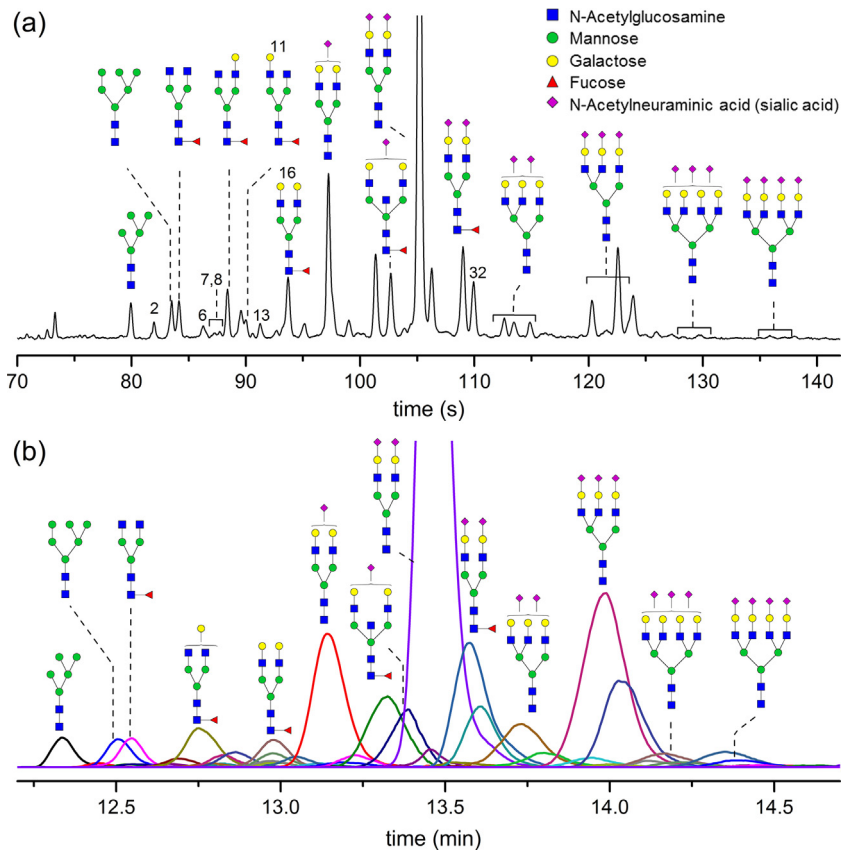

Fig. 1. (a) Electropherogram of methylamidated, APTS-labeled N-glycans derived from human serum and analyzed by microchip electrophoresis. N-Glycan structures were identified with electrophoretic mobility standards, enzymatic sequencing, and linkage isomer-specific derivatization with molecular weights determined by mass spectrometry. Peaks of the co-migrating species are numbered the same as in Table 1. (b) Extracted ion electropherogram of methylamidated, APTS-labeled N-glycans derived from human serum and analyzed by CE-MS.

Spectra, mass lists, and charge states obtained on the Orbitrap were exported as .CSV files for further analysis. For both methylamidated and lactonized/amidated serum samples, spectra were manually evaluated to determine the presence of low abundance species. Extracted ion electropherograms (EIE) for individual m/z values (±0.05 Da) from triplicate separations were boxcar averaged (7 or 11 point), exported, and normalized to total EIE peak area. The mass accuracy for this study ranged from 9 to 46 ppm after correction with m/z values from 11 known N-glycans in the same data set (Table S1 in the Supplementary Data).

2.5. Fabrication and operation of microfluidic devices

The microfluidic devices were fabricated in glass substrates [21,52] and had a serpentine channel with a 22-cm separation length and asymmetrically tapered, 180° turns [55]. To minimize electroosmotic flow and prevent sample adsorption, the microchannels were coated with linear poly(acrylamide). Samples were introduced into the analysis channel by modified pinched injections [21] and detected by laser-induced fluorescence with excitation from the 465-nm line of an argon ion laser (Melles Griot, Inc.). Peak areas and migration times were extracted from the electropherograms by fitting the peaks with a Gaussian function in OriginPro 2015.

2.6. MALDI-MS

For MALDI-MS analysis [56], methylamidated and permethylated N-glycan samples were interrogated in positive-ion mode by an SCIEX 4800 MALDI-TOF/TOF mass spectrometer in the m/z range from 1500 to 5000. Spectra were acquired from a total of 1000 laser shots for each sample, spotted in triplicate. Spectra were baseline-corrected, filtered, and converted to text files in Data Explorer 4.0. The data were normalized by expressing the intensity of each glycan ion as a percentage of the total intensity for all glycans in the spectra. N-Glycan structures and expected masses were drawn and calculated, respectively, with GlycoWorkBench software. Permethylated N-glycans had better ionization efficiencies than methylamidated N-glycans, generated better signal-to-noise ratios, and consequently, were used to compare across data sets.

3. Results and discussion

3.1. Microchip electrophoresis and CE-MS of serum N-glycans

APTS-labeled N-glycans were analyzed by both microchip electrophoresis (Fig. 1a) and CE-MS (Fig. 1b). The higher separation efficiency observed for the microchip electrophoresis is due, in part, to the narrow length injection, higher separation field strength (1250 V/cm), the separation channel coated with linear poly(acrylamide) to minimize adsorption of the N-glycans, and no hydrostatic pressure applied during the separation. Consequently, a number of N-glycans with structural isomers (i.e., positional and linkage isomers) are easily resolved by microchip electrophoresis and appear as multiple peaks because of differences in the hydrodynamic volumes of the isomers (Fig. 1a). These same structures appear as a single peak in the electropherogram for CE-MS (Fig. 1b) because of the lower separation efficiency on the commercial CE instrument.

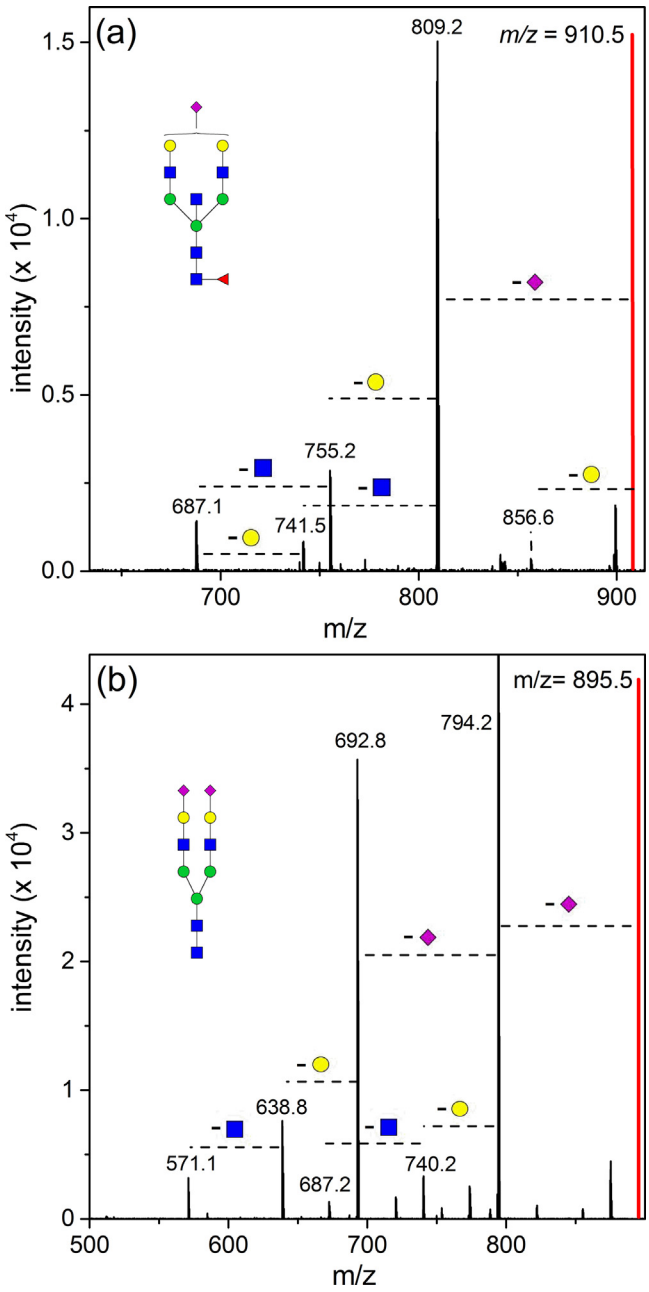

Fig. 2. MS/MS spectra for (a) $m/z = 910.5$ and (b) $m/z = 895.5$ ($z = -3$) (precursor ion indicated by the red line) at a normalized collision energy of 35. Y-type fragment losses and the resulting m/z values are indicated in the spectra. (For interpretation of the references to color in this figure legend, the reader is referred to the web version of this article.)

For CE-MS, we tested BGEs based on formic acid, acetic acid, ammonium formate, ammonium acetate, and ε-aminocaproic acid for the APTS-labeled glycan samples. BGEs with formic acid (0.05%–1%) and acetic acid (1%) both provided stable electrospray and reasonable separations. Optimal signal intensity was achieved with 0.1% formic acid with 10% IPA as the BGE. Separation efficiency and resolution improved with a decrease in sample concentration and injection length at the expense of overall signal in CE-MS experiments. With an injection of 15 s at 5 psi, severe peak distortion was observed, whereas decreasing the injection to 5 s at 1 psi resulted in reasonably efficient separation (Fig. 1b), but with a decrease in the overall signal intensity of ~8 times. However, these longer injections benefited MS/MS analysis of low abundance species.

Methylamidated, APTS-labeled N-glycans were introduced into the Orbitrap mass spectrometer via electrospray ionization after being electrophoretically separated in a bare fused silica capillary. For MS analysis, the primary charge state for most APTS-labeled N-glycans was $z = -3$ (charge of APTS), but N-glycans with total masses <2100 Da, including the mass of APTS, also exhibited $z = -2$ because these ions picked up a proton from the BGE (pH 2.8). Electropherograms for individual m/z values with $z = -2$ and -3 corresponding to each expected N-glycan were exported and overlaid to produce the extracted ion electropherogram (EIE) of N-glycans in Fig. 1b.

Mass spectra were collected in negative ion mode due to the negatively charged APTS label used to give the neutralized N-glycans a charge for electrophoretic separation. This mode proved to be beneficial for structural identification because negative

mode MS produces less complicated spectra than positive mode [34–36,57]. Moreover, the −3 charge on each N-glycan also creates a unique signature for labeled species to aid in differentiating them from the background. To confirm peak assignments, peak order and relative abundances were compared for all N-glycans identified in electropherograms from both microchip and capillary separations. In all cases, assignments of non-bisected and bisected glycans from microchip electrophoresis were in good agreement with the CE-MS experiments.

3.2. Analysis of co-migrating N-glycans

A shortcoming to structural identification by electrophoretic mobility standards is determining the relative intensities of N-glycans with overlapping migration times. Several N-glycans appeared to co-migrate in our microfluidic separations; however, their relative intensities were unknown due to our inability to isolate each N-glycan. These glycans were subsequently analyzed by CE-MS to determine their presence in serum, relative abundance, and electrophoretic mobility. This direct structural identification also allowed us to uncover N-glycans that may have been masked by species with similar mobilities. In total, seven sets of co-migrating species were identified with electrophoretic mobility standards (Table 1). Analysis of these *m*/*z* values with CE-MS positively confirmed the presence of all species but also provided the relative abundances of each N-glycan, if comparable ionization efficiencies are assumed.

3.3. Analysis of unidentified m/z values

Direct structural identification through CE-MS analysis helped us to identify new *m*/*z* values that correspond to potential N-glycan structures in serum. Masses found in spectra of methylamidated N-glycans from serum that did not correspond to a previously identified N-glycan were compiled, and five lists of possible native masses corresponding to neutral through tetra-sialylated species were generated. These mass lists were compared to an ExPasy GlycoMod database (http://web.expasy.org/glycomod) to generate lists of potential N-glycan structures. These structures were then refined based on the presence of the tri-mannosyl core, 0–3 fucosyl groups, and standard GlcNAc and Gal ordering.

This analysis yielded thirty-one new structures (see Table 2), not previously identified by microchip electrophoresis and electrophoretic mobility standards. For example, two disialylated, bifucosylated N-glycans ($[1114]^{3-}$ and $[1236]^{3-}$ in Table 2) were found in the database and likely to be in the serum samples. Their estimated migration times, which are calculated through electrophoretic mobility standards for APTS-labeled N-glycans [39], correspond to N-glycan peaks from serum samples that do not have assigned structures, and the relative peak areas between the capillary and microchip separations are in good agreement. Furthermore, the mass corresponding to $[1114]^{3-}$ also appears in the MALDI-MS spectrum of permethylated serum N-glycans. Criteria for structural assignment included: presence of a tri-mannosyl core, 0–3 fucosyl groups, and alternating GlcNAc and Gal monosaccharides to extend the antennae. For mass $[882]^{3-}$, the bolded composition in line 5 of Table 2 corresponds to a structure that fits the above criteria, whereas the unbolded composition was rejected because the structure requires five fucoses (deoxyhexose). For other masses, only the structural compositions fitting the above criteria are listed. Observed *m*/*z* values were corrected with a linear calibration curve derived from observed/theoretical *m*/*z* ratios of 11 known N-glycans in the same data file (see Table S1). The corrected *m*/*z* values are also listed in Table 2.

3.4. MS/MS of serum N-glycans

After initial spectra were obtained for the full glycan profile, several N-glycan masses were selected for further structural analysis. Many of the N-glycan structures probed contained fucosyl or sialic acid groups, and MS/MS analysis was performed on these analytes to correlate expected structural losses with proposed structures, e.g., one sialic acid per antenna of a biantennary N-glycan instead of two sialic acids stacked on a single antenna (see Fig. 2).

Although previous reports [34–36] have shown that cross-ring fragmentation is the primary mode of fragmentation for negative ion mode, instead of glycosidic fragmentation in positive mode, we observed losses of full monosaccharides corresponding to Y-type ions [58] at a normalized collision energy of 35. This difference in the observed fragmentation is most likely due to the APTS label at the reducing end, which results in an open terminal ring structure at the reducing end [59,60]. Most MS/MS studies use software to facilitate fragment analysis [61], but these programs are set up for positive mode, permethylated analytes [62]; consequently, we analyzed the spectra manually. The emphasis here was to confirm the presence of specific monosaccharides and to obtain general structural information. Selected structures, masses, and fragmentation information are summarized in Table 3, and their corresponding spectra are shown in Fig. S1. Exhaustive MS/MS analysis [34–37] has been previously reported for desialylated and underivatized N-glycans to obtain positional isomer information, and other groups have shown that isomeric information can be obtained by MS^n analysis [38], photofragmentation methods [63], and drift time selection in IMS-CID-MS [64].

Negative-mode mass spectrometry reduces the tendency of fucosyl groups on N-glycans to be lost prematurely prior to detection, which allows antenna- versus core-linked fucoses to be distinguished [34,57]. Thus, we would not expect to see mass shifts for core-linked fucose groups in high abundance in MS/MS analysis, but rather, we would expect high fragmentation intensities for fucosyl losses from antenna linkages as monosaccharides are sequentially lost from the terminal end. The MS^2 *m*/*z* 741.5 (Fig. S1a and Table 3) shows fragments corresponding to loss of galactose (*m*/*z* 687.5) and fucose (*m*/*z* 638.82) residues, which could indicate the presence of a fucosyl group on an antenna, specifically linked to the galactose adjacent to N-acetylglucosamine. Fragmentation corresponding to the loss of a possibly antenna-linked fucose is also visible at *m*/*z* 692.83 (~10% relative intensity). No other fucosylated structures exhibited such high intensity for fucosyl losses, although several structures featured modest intensities. These low intensity fragmentation patterns could indicate that the rest of the fucosylated N-glycans either have core-based fucosyl linkages or only a very small percentage of their structural isomers contain an antennary fucose. Previous reports [46] support the presence of both core and antennae linkages; however, we currently do not have other experimental evidence of these fucosyl isomers.

In this work, we did not expect to observe fucose rearrangement because the glycans were negatively charged [57,65]. However, we were not able to conduct MS/MS analysis of many structures because of their low abundance and, therefore, could not confirm whether fucose rearrangement occurred. In addition to positional isomers of fucose, we believe that the combination of selectively labeling sialic acid linkages (see Lactonization section, below) and MS/MS with higher collision energies for cross-ring cleavages will be an effective method to obtain positional features and possible linkage information for all isomers present.

3.5. Charge neutralization through amidation or lactonization

In addition to neutralization by methylamidation, the native charges on serum N-glycans were also neutralized through a

Table 1
Peak area ratios for N-glycans identified as co-migrating in microchip electrophoresis (Fig. 1). Each ratio was calculated by dividing the peak area of the bolded *m/z* value (corresponding to the most intense peak in each group) by the less intense peak area(s).

peak number	N-glycan structures	nominal co-migrating *m/z* values (z = −3)	peak area ratio
2	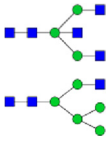	**652** 625	2.48
7 & 8	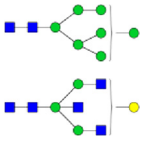	**665** 706	1.36
6	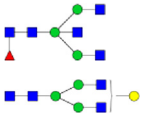	**701** 638	5.15
11	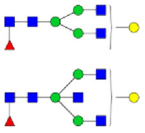	**687** 755	2.37
32	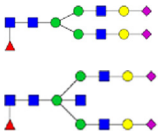	**944** 1011	2.66
16	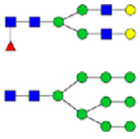	**741** 773	2.40
13	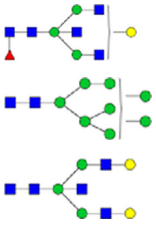	**755** 719 760	8.81:7.04:1 (755:719:760)

lactonization/amidation reaction. As previously reported [50,51], treatment of sialic acids with DMT-MM in the presence of ammonium chloride will amidate α2,6 linked sialic acids and spontaneously form intramolecular lactones with α2,3 linked sialic acids. We exploited this reaction to create unique masses based on the specific combination of α2,6 or α2,3 linkages present for different isomers of sialic acid-containing N-glycans. The lactone formation for α2,3 linked sialic acids and amidation of the α2,6 linked sialic acids also causes a migration shift for certain peaks in the electropherogram, further aiding with isomer identification. Fig. 3 compares microchip electropherograms of serum N-glycans that were methylamidated to serum N-glycans after lactonization/amidation. In the figure, black boxes highlight observed shifts in migration times for the methylamidated glycans with lower electrophoretic mobilities to the lactonized/amidated glycans with higher electrophoretic mobilities. As expected, the ring closure due to lactonization or addition of an amine group result in higher electrophoretic mobilities than addition of a methyl amine group. Additionally, the lactonized/amidated samples show several peaks with migration times <85 s, but the structures of these peaks have not been identified.

Possible linkages and the resulting mass shifts were calculated for each sialic acid-containing N-glycan, and experimental spectrum lists were compared to the expected lists to identify specific isomers. Each α2,6 linkage decreased ~1 Da, whereas the α2,3 linkage decreased by ~18 Da. These mass shifts result in unique *m/z* values for each combination of sialic acid linkages present for a given N-glycan (see Table 4). Additionally, the high mass accuracy of the Orbitrap mass spectrometer gives us a high degree of confidence for the accurate assignment of masses to specific N-glycan isomers. Large fluctuations in relative intensity were seen for the CE-MS analysis of lactonized/amidated serum samples with an average RSD for all samples of 34.3%. Peaks with <1% normalized intensities had a higher average RSD at 37.5%, whereas peaks with

Table 2
Observed, corrected, and theoretical *m/z* values, potential compositions and structures, and calculated migration times (field strength of 1250 V/cm) for *m/z* values found in spectra of methylamidated N-glycans from serum. These structures were not previously identified in our experiments with MALDI-MS and microchip electrophoresis with electrophoretic mobility standards. The corrected *m/z* values were calculated from *m/z* ratios observed for 11 known N-glycans from the same data set (Table S1).

observed *m/z* (z = −3)	corrected *m/z* (z = −3)	theoretical *m/z* (z = −3)	potential composition	potential structure	calculated migration time (s)
no sialic acids					
571.1332	571.2947	571.3043	$(Hex)_1$ $(HexNAc)_1$ + $(Man)_3(GlcNAc)_2$		83.52
584.8128	584.9742	584.9798	$(HexNAc)_2$ + $(Man)_3(GlcNAc)_2$		84.35
619.8197	619.9809	619.9903	$(Hex)_1$ $(HexNAc)_1$ $(Deoxyhexose)_1$ + $(Man)_3(GlcNAc)_2$	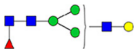	86.55
827.5457	827.7059	827.7168	$(Hex)_{10}$ + $(Man)_3(GlcNAc)_2$	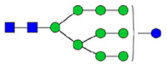	106.51
882.2415	882.4014	882.4184	**$(Hex)_3$ $(HexNAc)_4$ + $(Man)_3(GlcNAc)_2$**	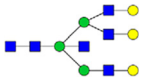	109.31
			$(Hex)_1$ $(HexNAc)_2$ $(Deoxyhexose)_5$ + $(Man)_3(GlcNAc)_2$		
1 sialic acid					
721.1950	721.3557	721.3721	$(Hex)_1$ $(HexNAc)_1$ $(Deoxyhexose)_1$ $(NeuAc)_1$ + $(Man)_3(GlcNAc)_2$	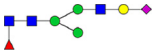	93.60
807.8952	808.0555	808.0790	$(Hex)_1$ $(HexNAc)_3$ $(NeuAc)_1$ + $(Man)_3(GlcNAc)_2$	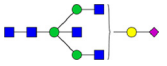	96.23
891.5913	891.7512	891.7755	$(Hex)_2$ $(HexNAc)_2$ $(Deoxyhexose)_2$ $(NeuAc)_1$ + $(Man)_3(GlcNAc)_2$	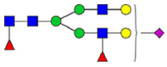	108.47
1032.3083	1032.4675	1032.4834	$(Hex)_3$ $(HexNAc)_4$ $(Deoxyhexose)_1$ $(NeuAc)_1$ + $(Man)_3(GlcNAc)_2$	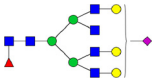	117.81
1037.6460	1037.8052	1037.8250	$(Hex)_4$ $(HexNAc)_4$ $(NeuAc)_1$ + $(Man)_3(GlcNAc)_2$	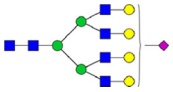	118.13
1086.3235	1086.4824	1086.5110	$(Hex)_4$ $(HexNAc)_4$ $(Deoxyhexose)_1$ $(NeuAc)_1$ + $(Man)_3(GlcNAc)_2$	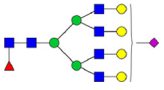	121.20
2+ sialic acids					
1114.6460	1114.8048	1114.8558	$(Hex)_3$ $(HexNAc)_3$ $(Deoxyhexose)_2$ $(NeuAc)_2$ + $(Man)_3(GlcNAc)_2$	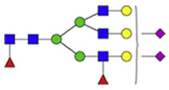	123.06
1236.3838	1236.5420	1236.5665	$(Hex)_4$ $(HexNAc)_4$ $(Deoxyhexose)_2$ $(NeuAc)_2$ + $(Man)_3(GlcNAc)_2$	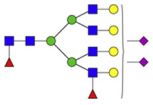	132.07
1220.0636	1220.2219	1220.2419	$(Hex)_3$ $(HexNAc)_3$ $(NeuAc)_4$ + $(Man)_3(GlcNAc)_2$	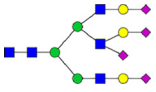	130.50
1235.0607	1235.2189	1235.2503	$(Hex)_3$ $(HexNAc)_4$ $(NeuAc)_3$ + $(Man)_3(GlcNAc)_2$	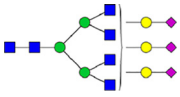	131.63
1260.7155	1260.8735	1260.9109	$(Hex)_5$ $(HexNAc)_5$ $(NeuAc)_2$ + $(Man)_3(GlcNAc)_2$	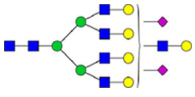	133.62
1309.4263	1309.5841	1309.5968	$(Hex)_5$ $(HexNAc)_5$ $(Deoxyhexose)_1$ $(NeuAc)_2$ + $(Man)_3(GlcNAc)_2$	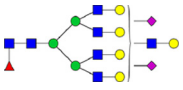	137.55

Table 2 (*Continued*)

observed	corrected	theoretical	potential composition	potential structure	calculated migration time (s)
1337.7569	1337.9146	1337.9456	$(Hex)_4$ $(HexNAc)_4$ $(Deoxyhexose)_2$ $(NeuAc)_3 + (Man)_3(GlcNAc)_2$	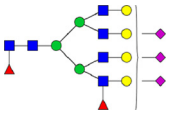	139.95
1362.1039	1362.2614	1362.2927	$(Hex)_5$ $(HexNAc)_5$ $(NeuAc)_3 + (Man)_3(GlcNAc)_2$	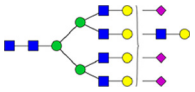	142.08
1386.4431	1386.6005	1386.6315	$(Hex)_4$ $(HexNAc)_4$ $(Deoxyhexose)_3$ $(NeuAc)_3 + (Man)_3(GlcNAc)_2$	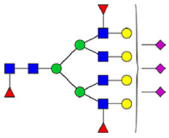	144.2779
1410.7789	1410.9362	1410.9786	$(Hex)_5$ $(HexNAc)_5$ $(Deoxyhexose)_1$ $(NeuAc)_3 + (Man)_3(GlcNAc)_2$	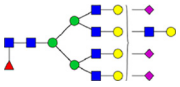	146.54
1439.1362	1439.2934	1439.3263	$(Hex)_4$ $(HexNAc)_4$ $(Deoxyhexose)_2$ $(NeuAc)_4 + (Man)_3(GlcNAc)_2$	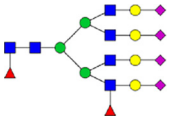	149.27
1459.4907	1459.6478	1459.6849	$(Hex)_5$ $(HexNAc)_5$ $(Deoxyhexose)_2$ $(NeuAc)_3 + (Man)_3(GlcNAc)_2$	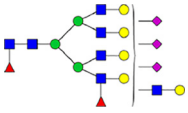	151.29
1463.4750	1463.6320	1463.6651	$(Hex)_5$ $(HexNAc)_5$ $(NeuAc)_4 + (Man)_3(GlcNAc)_2$	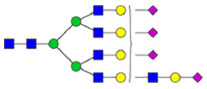	151.69
1487.8319	1487.9888	1488.0106	$(Hex)_4$ $(HexNAc)_4$ $(Deoxyhexose)_3$ $(NeuAc)_4 + (Man)_3(GlcNAc)_2$	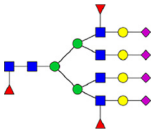	154.20
1512.1360	1512.2928	1512.3511	$(Hex)_5$ $(HexNAc)_5$ $(Deoxyhexose)_1$ $(NeuAc)_4 + (Man)_3(GlcNAc)_2$	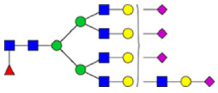	156.78
1560.8510	1561.0076	1560.9797	$(Hex)_5$ $(HexNAc)_5$ $(Deoxyhexose)_2$ $(NeuAc)_4 + (Man)_3(GlcNAc)_2$	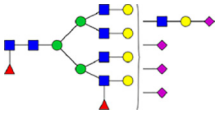	162.22
1585.1838	1585.3402	1585.3759	$(Hex)_6$ $(HexNAc)_6$ $(NeuAc)_4 + (Man)_3(GlcNAc)_2$	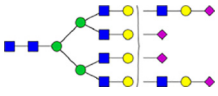	165.10
1609.5139	1609.6702	1609.7213	$(Hex)_5$ $(HexNAc)_5$ $(Deoxyhexose)_3$ $(NeuAc)_4 + (Man)_3(GlcNAc)_2$	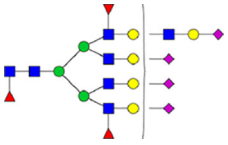	168.07
1633.8810	1634.0372	1634.0878	$(Hex)_6$ $(HexNAc)_6$ $(Deoxyhexose)_1$ $(NeuAc)_4 + (Man)_3(GlcNAc)_2$	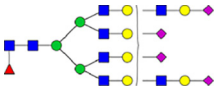	171.15
1686.5778	1686.7337	1686.7631	$(Hex)_6$ $(HexNAc)_6$ $(NeuAc)_5 + (Man)_3(GlcNAc)_2$	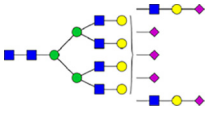	178.22

Table 3
Selected N-glycan structures, calculated m/z values with $z = -3$, m/z values for MS/MS fragmentation, relative intensity of each fragment, and corresponding monosaccharide losses. All parent ions listed were analyzed with the FTMS mass analyzer except for $m/z = 1167$, which was analyzed with the ITMS mass analyzer due to low ion intensity.

structure	calculated m/z	fragmentation m/z	relative intensity	structural loss
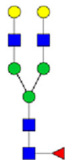	741.5321	692.834 687.50 638.82 633.49 619.81	10.39 94.18 95.11 5.16 27.73	Fucose Gal Gal + Fucose 2 Gal Gal + GlcNAc
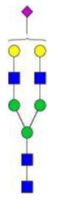	794.2146	740.19 692.84 638.82 584.80 571.13 517.11	5.46 100 27.60 2.74 9.66 2.05	Gal SA SA +Gal SA + 2 Gal SA + Gal +GlcNAc SA + 2 Gal + GlcNAc
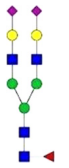	944.2794	842.75 (794.55) 788.88 741.52 (692.84) 687.51	91.31 (0.62) 3.80 60.83 (1.05) 11.15	SA (+Fucose) SA + Gal 2SA (+Fucose) 2SA + Gal
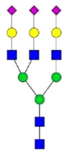	1118.669	1017.29 963.28 915.92 861.90 814.54 760.53	77.08 2.44 59.47 5.79 22.48 4.87	SA SA + Gal 2SA 2SA + Gal 3SA 3SA + Gal
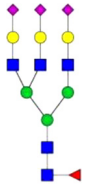	1167.335	1118.68 1066.17 (1017.33) 965.083 (916.42) 863.33 (814.50) 910.58 (861.92) 809.17 (760.67) 755.17	0.62 72.13 (1.57) 68.27 (3.77) 16.51 (0.68) 2.96 (0.27) 1.47 (0.46) 0.30	Fucose SA (+Fucose) 2SA (+Fucose) 3SA(+Fucose) 2SA + Gal (+Fucose) 3 SA + Gal (+Fucose) 3 SA + 2 Gal

>1% normalized intensities had a lower average RSD at 28.7%. These results are consistent with previously reported fluctuations [51] of lactonized/amidated N-glycans.

For monosialylated N-glycans, the α2,6 linkage is dominant for every species. Several species were only present with α2,6 linkages, and with both α2,3 and α2,6 linkages present, the α2,6 linkage was the dominant linkage. This finding is in good agreement with previous research that shows the predominant expression of α2,6 linkages. Di-sialylated N-glycans with both sialic acids having α2,6 linkages are again dominant, but dual α2,3 linkages were second most abundant for several species, which is also in good agreement with other reported abundances [51]. For several structures (e.g., biantennary and bisected), the di-α2,3 linked N-glycans would be almost symmetrical to di-α2,6 linked N-glycans, making them difficult to separate with electrophoresis. However, the unique masses associated with specific linkage isomers after treatment with DMT-MM in ammonium chloride allows us to identify these previously unseen structures.

The analysis of triantennary and larger structures poses unique challenges to the identification of specific sialic acid linkages due to their low abundance in serum. However, m/z values corresponding to all α2,6 linkages were identified in all of the larger N-glycans previously identified except for the tetra-antennary, tetra-sialylated, fucosylated structure. Many of these larger structures (e.g., the isomer at m/z 1087) exhibit an extremely low fraction of α2,3 linked sialic acids which does not agree with earlier reported abundances [51] or our own glycosidase digestions. Lactones may not be sufficiently stable and could hydrolyze prior to analysis to regenerate the carboxyl group of sialic acid [66], consequently forming amides by reacting with surrounding ammonium chloride. Thus, a small portion of α2,3 linked sialic acid lactones could appear as amides, which would give a slightly higher apparent abundance of α2,6 linked sialic acid isomers. Incubating at 60 °C for 17 h was found to be optimal, as most of the sialylated N-glycans were neutralized successfully through this strategy without a large bias in lactone/amide ratio.

In addition to linkage isomers, positional isomers also contribute to the complexity of the N-glycome. Several methods exist to elucidate these isomers (e.g., enzymatic profiling [30,67] and MS^n [34–38,57,61,63]), but these approaches are time consuming and difficult to analyze for a sample set as complex as serum. Our early attempts with enzymatic cleavage lacked the specificity to

Table 4
Possible linkage isomers present for sialylated N-glycans from serum. Listed for each structure are the theoretical m/z, number of α2,3 and α2,6 linkages, and normalized and relative peak areas.

structure	theoretical m/z (z = −3)	# α2,3	# α2,6	normalized apparent peak area	relative apparent peak area
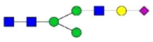	661.962	1	0	–	–
	667.639	0	1	0.03	1.07E-04
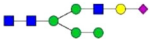	715.979	1	0	0.07	3.40E-04
	721.656	0	1	0.13	6.09E-04
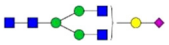	726.655	1	0	–	–
	735.332	0	1	0.29	1.36E-03
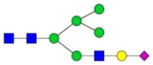	769.997	1	0	–	–
	775.674	0	1	0.23	9.13E-04
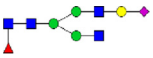	778.341	1	0	0.12	5.35E-04
	784.018	0	1	0.60	2.95E-03
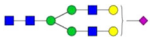	783.672	1	0	0.16	4.65E-04
	789.349	0	1	21.55	6.99E-02
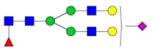	832.358	1	0	0.13	5.23E-04
	838.035	0	1	8.85	4.25E-02
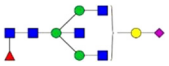	846.034	1	0	–	–
	851.711	0	1	0.51	2.03E-03
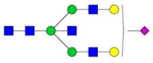	851.366	1	0	0.04	1.85E-04
	857.043	0	1	1.57	5.02E-03
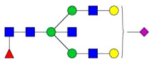	900.052	1	0	–	–
	905.729	0	1	1.57	2.64E-02
	905.383	1	0	–	–
	911.060	0	1	8.17	1.09E-02
	954.069	1	0	0.48	1.58E-03
	959.746	0	1	1.02	4.21E-03
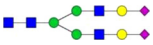	874.699	2	0	0.35	1.06E-03
	880.376	1	1	0.72	2.44E-03
	886.053	0	2	100.00	3.24E-01
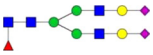	923.358	2	0	4.97	1.64E-02
	929.062	1	1	1.39	4.49E-03
	934.739	0	2	18.37	6.43E-02
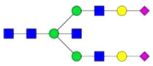	942.392	2	0	0.21	3.75E-04
	948.069	1	1	0.07	1.94E-04
	953.746	0	2	0.48	1.59E-03
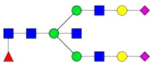	991.078	2	0	0.20	6.67E-04
	996.755	1	1	0.09	3.52E-04
	1002.432	0	2	8.73	2.86E-02
	996.410	2	0	0.44	2.34E-03
	1002.087	1	1	0.15	4.90E-04
	1007.764	0	2	11.30	3.70E-02
	1045.096	2	0	0.59	1.45E-03
	1050.773	1	1	0.23	7.65E-04
	1056.450	0	2	4.49	1.48E-02
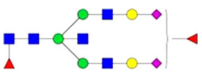	1039.764	2	0	–	–
	1045.441	1	1	0.59	1.93E-03
	1051.118	0	2	–	–
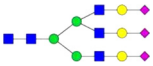	1087.437	3	0	0.01	–
	1093.114	2	1	0.21	1.00E-03
	1098.791	1	2	6.47	1.63E-02
	1104.468	0	3	43.88	1.85E-01
	1136.123	3	0	0.49	1.50E-03
	1141.800	2	1	1.63	5.30E-03
	1147.477	1	2	2.20	7.16E-03
	1153.154	0	3	7.75	2.37E-02
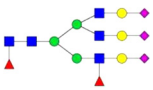	1184.809	3	0	–	2.89E-02
	1190.486	2	1	0.49	1.63E-03
	1196.163	1	2	0.34	1.12E-03
	1201.840	0	3	0.47	1.52E-03

Table 4 (*Continued*)

structure	theoretical m/z ($z=-3$)	# α2,3	# α2,6	normalized apparent peak area	relative apparent peak area
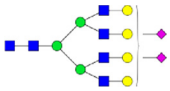	1118.121	2	0	–	–
	1123.798	1	1	0.71	2.46E-03
	1129.475	0	2	1.72	5.44E-03
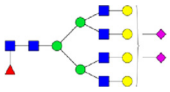	1166.807	2	0	0.22	6.69E-04
	1172.484	1	1	–	–
	1178.161	0	2	1.35	6.13E-03
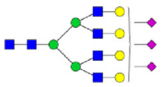	1209.148	3	0	–	–
	1214.825	2	1	0.06	2.05E-04
	1220.502	1	2	1.79	8.42E-03
	1226.179	0	3	1.00	4.83E-03
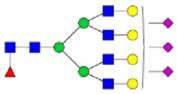	1257.834	3	0	–	–
	1263.511	2	1	0.08	2.87E-04
	1269.188	1	2	0.18	5.92E-04
	1274.865	0	3	0.47	1.46E-03
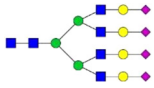	1300.174	4	0	–	–
	1305.851	3	1	–	–
	1311.528	2	2	–	–
	1317.205	1	3	0.44	1.41E-03
	1322.882	0	4	4.09	1.98E-02
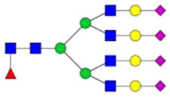	1348.860	4	0	0.31	1.20E-03
	1354.537	3	1	–	–
	1360.214	2	2	–	–
	1365.891	1	3	–	–
	1371.568	0	4	–	–

give conclusive results, and the use of methylamidation instead of permethylation renders MS/MS data analysis unsuitable for currently available automated data processing resources. Thus, our use of negative mode and non-traditional modification reactions makes manual evaluation necessary to correlate specific losses with exact positional information.

4. Conclusion

Continuation of our work to unambiguously identify N-glycans in serum led us to analyze samples with a CE-MS instrument interfaced with a Thermo Orbitrap. The results obtained from this direct identification method included confirmation of N-glycan masses proposed from prior experiments with electrophoretic mobility standards, observation of expected monosaccharide loss patterns through MS/MS analysis, proposal of thirty-one previously unidentified N-glycan structures, and identification of specific sialic acid linkages. These results confirm the validity of our previous results obtained through indirect identification methods and also further our understanding of sialic acid linkages. Future efforts will focus on increasing signal intensity and using higher collision energies to generate cross-ring cleavages and determine linkage isomers to further refine structural isomer assignments.

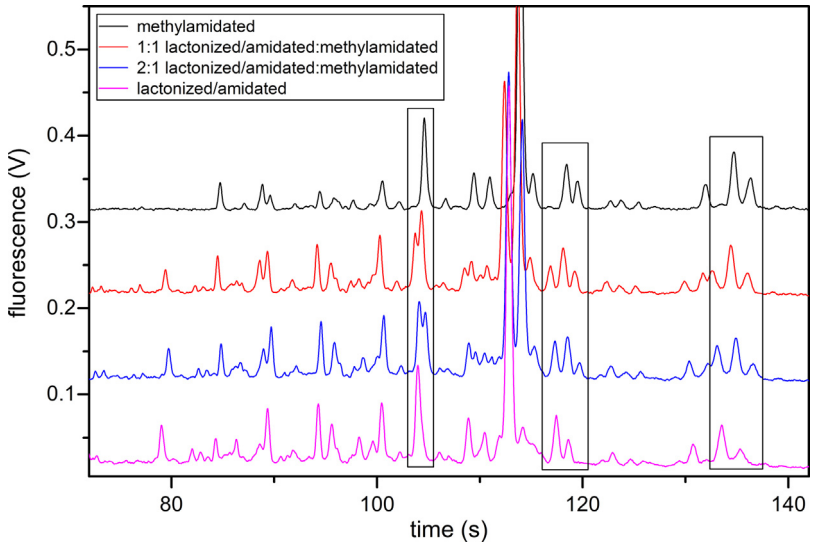

Fig. 3. Electropherograms of methylamidated and lactonized/amidated N-glycans derived from serum and mixtures of them that were analyzed by microchip electrophoresis. The black boxes highlight three examples of observed shifts in migration times for the methylamidated glycans with lower electrophoretic mobilities (top trace) to the lactonized/amidated glycans with higher electrophoretic mobilities (bottom trace).

Acknowledgement

This work was supported in part by grant NIH R01 GM106084. The authors thank the Indiana University Nanoscale Characterization Facility for use of its instruments.

Appendix A. Supplementary data

Supplementary data associated with this article can be found, in the online version, at http://dx.doi.org/10.1016/j.chroma.2017.09.009.

References

[1] J.W. Dennis, M. Granovsky, C.E. Warren, Protein glycosylation in development and disease, Bioessays 21 (1999) 412–421.
[2] D.H. Dube, C.R. Bertozzi, Glycans in cancer and inflammation. Potential for therapeutics and diagnostics, Nat. Rev. Drug Discov. 4 (2005) 477–488.
[3] S. Hakomori, Tumor malignancy defined by aberrant glycosylation and sphingo(glyco)lipid metabolism, Cancer Res. 56 (1996) 5309–5318.
[4] A. Kobata, A retrospective and prospective view of glycopathology, Glycoconj. J. 15 (1998) 323–331.
[5] C. Kirmiz, B.S. Li, H.J. An, B.H. Clowers, H.K. Chew, K.S. Lam, A. Ferrige, R. Alecio, A.D. Borowsky, S. Sulaimon, C.B. Lebrilla, S. Miyamoto, A serum glycomics approach to breast cancer biomarkers, Mol. Cell. Proteom. 6 (2007) 43–55.
[6] Z. Kyselova, Y. Mechref, P. Kang, J.A. Goetz, L.E. Dobrolecki, G.W. Sledge, L. Schnaper, R.J. Hickey, L.H. Malkas, M.V. Novotny, Breast cancer diagnosis and prognosis through quantitative measurements of serum glycan profiles, Clin. Chem. 54 (2008) 1166–1175.
[7] U.M. Abd Hamid, L. Royle, R. Saldova, C.M. Radcliffe, D.J. Harvey, S.J. Storr, M. Pardo, R. Antrobus, C.J. Chapman, N. Zitzmann, J.F. Robertson, R.A. Dwek, P.M. Rudd, A strategy to reveal potential glycan markers from serum glycoproteins associated with breast cancer progression, Glycobiology 18 (2008) 1105–1118.
[8] J.A. Goetz, Y. Mechref, P. Kang, M.H. Jeng, M.V. Novotny, Glycomic profiling of invasive and non-invasive breast cancer cells, Glycoconj. J. 26 (2009) 117–131.
[9] A. Pierce, R. Saldova, U.M. Abd Hamid, J.L. Abrahams, E.W. McDermott, D. Evoy, M.J. Duffy, P.M. Rudd, Levels of specific glycans significantly distinguish lymph node-positive from lymph node-negative breast cancer patients, Glycobiology 20 (2010) 1283–1288.
[10] H.J. An, S. Miyamoto, K.S. Lancaster, C. Kirmiz, B.S. Li, K.S. Lam, G.S. Leiserowitz, C.B. Lebrilla, Profiling of glycans in serum for the discovery of potential biomarkers for ovarian cancer, J. Proteome Res. 5 (2006) 1626–1635.
[11] R. Saldova, L. Royle, C.M. Radcliffe, U.M.A. Hamid, R. Evans, J.N. Arnold, R.E. Banks, R. Hutson, D.J. Harvey, R. Antrobus, S.M. Petrescu, R.A. Dwek, P.M. Rudd, Ovarian cancer is associated with changes in glycosylation in both acute-phase proteins and IgG, Glycobiology 17 (2007) 1344–1356.
[12] G. Tabares, C.M. Radcliffe, S. Barrabes, M. Ramirez, R.N. Aleixandre, W. Hoesel, R.A. Dwek, P.M. Rudd, R. Peracaula, R. de Llorens, Different glycan structures in prostate-specific antigen from prostate cancer sera in relation to seminal plasma PSA, Glycobiology 16 (2006) 132–145.
[13] Z. Kyselova, Y. Mechref, M.M. Al Bataineh, L.E. Dobrolecki, R.J. Hickey, J. Vinson, C.J. Sweeney, M.V. Novotny, Alterations in the serum glycome due to metastatic prostate cancer, J. Proteome Res. 6 (2007) 1822–1832.
[14] R. Goldman, H.W. Ressom, R.S. Varghese, L. Goldman, G. Bascug, C.A. Loffredo, M. Abdel-Hamid, I. Gouda, S. Ezzat, Z. Kyselova, Y. Mechref, M.V. Novotny, Detection of hepatocellular carcinoma using glycomic analysis, Clin. Cancer Res. 15 (2009) 1808–1813.
[15] A.S. Vercoutter-Edouart, M.C. Slomianny, O. Dekeyzer-Beseme, J.F. Haeuw, J.C. Michalski, Glycoproteomics and glycomics investigation of membrane N-glycosylproteins from human colon carcinoma cells, Proteomics 8 (2008) 3236–3256.
[16] J. Zhao, D.M. Simeone, D. Heidt, M.A. Anderson, D.M. Lubman, Comparative serum glycoproteomics using lectin selected sialic acid glycoproteins with mass spectrometric analysis: application to pancreatic cancer serum, J. Proteome Res. 5 (2006) 1792–1802.
[17] J. Zhao, W.L. Qiu, D.M. Simeone, D.M. Lubman, N-linked glycosylation profiling of pancreatic cancer serum using capillary liquid phase separation coupled with mass spectrometric analysis, J. Proteome Res. 6 (2007) 1126–1138.
[18] Y. Mechref, A. Hussein, S. Bekesova, V. Pungpapong, M. Zhang, L.E. Dobrolecki, R.J. Hickey, Z.T. Hammoud, M.V. Novotny, Quantitative serum glycomics of esophageal adenocarcinoma and other esophageal disease onsets, J. Proteome Res. 8 (2009) 2656–2666.
[19] F.Q. Dang, L.H. Zhang, M. Jabasini, N. Kaji, Y. Baba, Characterization of electrophoretic behavior of sugar isomers by microchip electrophoresis coupled with videomicroscopy, Anal. Chem. 75 (2003) 2433–2439.
[20] D. Vanderschaeghe, A. Szekrenyes, C. Wenz, M. Gassmann, N. Naik, M. Bynum, H.F. Yin, J. Delanghe, A. Guttman, N. Callewaert, High-throughput profiling of the serum N-glycome on capillary electrophoresis microfluidics systems: toward clinical implementation of glycohepatotest, Anal. Chem. 82 (2010) 7408–7415.
[21] Z. Zhuang, J.A. Starkey, Y. Mechref, M.V. Novotny, S.C. Jacobson, Electrophoretic analysis of N-glycans on microfluidic devices, Anal. Chem. 79 (2007) 7170–7175.
[22] Z. Zhuang, I. Mitra, A. Hussein, M.V. Novotny, Y. Mechref, S.C. Jacobson, Microchip electrophoresis of N-glycans on serpentine separation channels with asymmetrically tapered turns, Electrophoresis 32 (2011) 246–253.
[23] I. Mitra, Z. Zhuang, Y. Zhang, C.-Y. Yu, Z.T. Hammoud, H. Tang, Y. Mechref, S.C. Jacobson, N-glycan profiling by microchip electrophoresis to differentiate disease states related to esophageal adenocarcinoma, Anal. Chem. 84 (2012) 3621–3627.
[24] J.P. Liu, O. Shirota, D. Wiesler, M. Novotny, Ultrasensitive fluorometric detection of carbohydrates as derivatives in mixtures separated by capillary electrophoresis, Proc. Natl. Acad. Sci. U. S. A. 88 (1991) 2302–2306.
[25] W. Nashabeh, Z. El Rassi, Capillary zone electrophoresis of linear and branched oligosaccharides, J. Chromatogr. A 600 (1992) 279–287.
[26] K. Kakehi, A. Susami, A. Taga, S. Suzuki, S. Honda, High-performance capillary electrophoresis of O-glycosidically linked sialic acid-containing oligosaccharides in glycoproteins as their alditol derivatives with low-wavelength UV monitoring, J. Chromatogr. A 680 (1994) 209–215.
[27] N. Callewaert, R. Contreras, L. Mitnik-Gankin, L. Carey, P. Matsudaira, D. Ehrlich, Total serum protein N-glycome profiling on a capillary electrophoresis-microfluidics platform, Electrophoresis 25 (2004) 3128–3131.
[28] R.J. Luo, S.A. Archer-Hartmann, L.A. Holland, Transformable capillary electrophoresis for oligosaccharide separations using phospholipid additives, Anal. Chem. 82 (2010) 1228–1233.
[29] S.A. Archer-Hartmann, L.M. Sargent, D.T. Lowry, L.A. Holland, Microscale exoglycosidase processing and lectin capture of glycans with phospholipid assisted capillary electrophoresis separations, Anal. Chem. 83 (2011) 2740–2747.
[30] S. Mittermayr, J. Bones, M. Doherty, A. Guttman, P.M. Rudd, Multiplexed analytical glycomics: rapid and confident igg N-glycan structural elucidation, J. Proteome Res. 10 (2011) 3820–3829.
[31] S. Mittermayr, A. Guttman, Influence of molecular configuration and conformation on the electromigration of oligosaccharides in narrow bore capillaries, Electrophoresis 33 (2012) 1000–1007.
[32] A. Guttman, K.W. Ulfelder, Exoglycosidase matrix-mediated sequencing of a complex glycan pool by capillary electrophoresis, J. Chromatogr. A 781 (1997) 547–554.
[33] K. Yamashita, T. Mizuochi, A. Kobata, Analysis of oligosaccharides by gel-filtration, Methods Enzymol. 83 (1982) 105–126.
[34] D.J. Harvey, Fragmentation of negative ions from carbohydrates: part 3. Fragmentation of hybrid and complex N-linked glycans, J. Am. Soc. Mass Spectrom. 16 (2005) 647–659.
[35] D.J. Harvey, Fragmentation of negative ions from carbohydrates: part 2. Fragmentation of high-mannose N-linked glycans, J. Am. Soc. Mass Spectrom. 16 (2005) 631–646.
[36] D.J. Harvey, Fragmentation of negative ions from carbohydrates: part 1. Use of nitrate and other anionic adducts for the production of negative ion electrospray spectra from N-linked carbohydrates, J. Am. Soc. Mass Spectrom. 16 (2005) 622–630.
[37] D.J. Harvey, M. Crispin, C. Scanlan, B.B. Singer, L. Lucka, V.T. Chang, C.M. Radcliffe, S. Thobhani, C.T. Yuen, P.M. Rudd, Differentiation between isomeric triantennary N-linked glycans by negative ion tandem mass spectrometry and confirmation of glycans containing galactose attached to the bisecting (beta 1–4-Glcnac) residue in N-glycans from igg, Rapid Commun. Mass Spectrom. 22 (2008) 1047–1052.
[38] D.J. Ashline, A.J. Lapadula, Y.H. Liu, M. Lin, M. Grace, B. Pramanik, V.N. Reinhold, Carbohydrate structural isomers analyzed by sequential mass spectrometry, Anal. Chem. 79 (2007) 3830–3842.
[39] I. Mitra, C.M. Snyder, X.M. Zhou, M.I. Campos, W.R. Alley, M.V. Novotny, S.C. Jacobson, Structural characterization of serum N-glycans by methylamidation, fluorescent labeling, and analysis by microchip electrophoresis, Anal. Chem. 88 (2016) 8965–8971.
[40] C.M. Snyder, W.R. Alley, M.I. Campos, M. Svoboda, J.A. Goetz, J.A. Vasseur, S.C. Jacobson, M.V. Novotny, Complementary glycomic analyses of sera derived from colorectal cancer patients by MALDI-Tof-Ms and microchip electrophoresis, Anal. Chem. 88 (2016) 9597–9605.
[41] X.F. Zhong, Z.C. Zhang, S. Jiang, L.J. Li, Recent advances in coupling capillary electrophoresis- based separation techniques to ESI and MALDI-Ms, Electrophoresis 35 (2014) 1214–1225.
[42] J.A. Olivares, N.T. Nguyen, C.R. Yonker, R.D. Smith, Online mass-spectrometric detection for capillary zone electrophoresis, Anal. Chem. 59 (1987) 1230–1232.
[43] M. Moini, Simplifying Ce-Ms operation. 2. Interfacing low-flow separation techniques to mass spectrometry using a porous tip, Anal. Chem. 79 (2007) 4241–4246.
[44] J.S. Mellors, V. Gorbounov, R.S. Ramsey, J.M. Ramsey, Fully integrated glass microfluidic device for performing high-efficiency capillary electrophoresis and electrospray ionization mass spectrometry, Anal. Chem. 80 (2008) 6881–6887.
[45] R. Wojcik, O.O. Dada, M. Sadilek, N.J. Dovichi, Simplified capillary electrophoresis nanospray sheath-flow interface for high efficiency and sensitive peptide analysis, Rapid Commun. Mass Spectrom. 24 (2010) 2554–2560.

[46] J.A. Vasseur, J.A. Goetz, W.R. Alley, M.V. Novotny, Smoking and lung cancer-induced changes in N-glycosylation of blood serum proteins, Glycobiology 22 (2012) 1684–1708.
[47] X. Liu, H. Qiu, R.K. Lee, W. Chen, J. Li, Methylamidation for sialoglycomics by MALDI-MS: a facile derivatization strategy for both alpha 2,3-and alpha 2,6-linked sialic acids, Anal. Chem. 82 (2010) 8300–8306.
[48] M. Kunishima, C. Kawachi, K. Hioki, R. Terao, S. Tani, Formation of carboxamides by direct condensation of carboxylic acids and amines in alcohols using a new alcohol- and water-soluble condensing agent: DMT-MM, Tetrahedron 57 (2001) 1551–1558.
[49] M. Kunishima, J. Morita, C. Kawachi, F. Iwasaki, K. Terao, S. Tani, Esterification of carboxylic acids with alcohols by 4-(4,6-dimethoxy-1,3,5-triazin-2-Yl) −4-methyl-morpholinium chloride (DMTMM), Synlett (1999) 1255–1256.
[50] S. Sekiya, Y. Wada, K. Tanaka, Derivatization for stabilizing sialic acids in MALDI-MS, Anal. Chem. 77 (2005) 4962–4968.
[51] W.R. Alley Jr., M.V. Novotny, Glycomic analysis of sialic acid linkages in glycans derived from blood serum glycoproteins, J. Proteome Res. 9 (2010) 3062–3072.
[52] I. Mitra, W.R. Alley, J.A. Goetz, J.A. Vasseur, M.V. Novotny, S.C. Jacobson, Comparative profiling of N-glycans isolated from serum samples of ovarian cancer patients and analyzed by microchip electrophoresis, J. Proteome Res. 12 (2013) 4490–4496.
[53] R.A. Evangelista, F.T.A. Chen, A. Guttman, Reductive amination of N-linked oligosaccharides using organic acid catalysts, J. Chromatogr. A 745 (1996) 273–280.
[54] M. Kunishima, C. Kawachi, J. Morita, K. Terao, F. Iwasaki, S. Tani, 4-(4,6-Dimethoxy-1,3,5-triazin-2-Yl)-4-methyl-morpholinium chloride: an efficient condensing agent leading to the formation of amides and esters, Tetrahedron 55 (1999) 13159–13170.
[55] J.D. Ramsey, S.C. Jacobson, C.T. Culbertson, J.M. Ramsey, High-efficiency, two-dimensional separations of protein digests on microfluidic devices, Anal. Chem. 75 (2003) 3758–3764.
[56] W.R. Alley, J.A. Vasseur, J.A. Goetz, M. Svoboda, B.F. Mann, D.E. Matei, N. Menning, A. Hussein, Y. Mechref, M.V. Novotny, N-linked glycan structures and their expressions change in the blood sera of ovarian cancer patients, J. Proteome Res. 11 (2012) 2282–2300.
[57] M. Wuhrer, A.M. Deelder, Negative-mode maldi-Tof/Tof-Ms of oligosaccharides labeled with 2-aminobenzamide, Anal. Chem. 77 (2005) 6954–6959.
[58] B. Domon, C.E. Costello, A systematic nomenclature for carbohydrate fragmentations in Fab-Ms Ms spectra of glycoconjugates, Glycoconj. J. 5 (1988) 397–409.
[59] D.J. Harvey, Collision-induced fragmentation of negative ions from N-linked glycans derivatized with 2-aminobenzoic acid, J. Mass Spectrom. 40 (2005) 642–653.
[60] T. Nishikaze, K. Kaneshiro, S. Kawabata, K. Tanaka, Structural analysis of N-glycans by the glycan-labeling method using 3-aminoquinoline-based liquid matrix in negative-ion MALDI-MS, Anal. Chem. 84 (2012) 9453–9461.
[61] K.L. Ford, W. Zeng, J.L. Heazlewood, A. Bacic, Characterization of protein N-glycosylation by tandem mass spectrometry using complementary fragmentation techniques, Front. Plant Sci. 6 (2015) 00674.
[62] Y.L. Hu, S.Y. Zhou, C.Y. Yu, H.X. Tang, Y. Mechref, Automated annotation and quantitation of glycans by liquid chromatography/electrospray ionization mass spectrometric analysis using the multiglycan-ESI computational tool, Rapid Commun. Mass Spectrom. 29 (2015) 135–142.
[63] A. Devakumar, Y. Mechref, P. Kang, M.V. Novotny, J.P. Reilly, Identification of isomeric N-glycan structures by mass spectrometry with 157 nm laser-induced photofragmentation, J. Am. Soc. Mass Spectrom. 19 (2008) 1027–1040.
[64] F.F. Zhu, S. Lee, S.J. Valentine, J.P. Reilly, D.E. Clemmer, Mannose7 glycan isomer characterization by Ims-Ms/Ms analysis, J. Am. Soc. Mass Spectrom. 23 (2012) 2158–2166.
[65] M. Wuhrer, C.A.M. Koeleman, C.H. Hokke, A.M. Deelder, Mass spectrometry of proton adducts of fucosylated N-glycans: fucose transfer between antennae gives rise to misleading fragments, Rapid Commun. Mass Spectrom. 20 (2006) 1747–1754.
[66] M. Pudelko, A. Lindgren, T. Tengel, C.A. Reis, M. Elofsson, J. Kihlberg, Formation of lactones from sialylated Muc1 glycopeptides, Org. Biomol. Chem. 4 (2006) 713–720.
[67] C. Schwedler, M. Kaup, S. Weiz, M. Hoppe, E.I. Braicu, J. Sehouli, B. Hoppe, R. Tauber, M. Berger, V. Blanchard, Identification of 34 N-glycan isomers in human serum by capillary electrophoresis coupled with laser-induced fluorescence allows improving glycan biomarker discovery, Anal. Bioanal. Chem. 406 (2014) 7185–7193.